JOURNAL OF COMPUTATIONAL PHYSICS 96, 325–338 (1991)

δf and Particle Simulations of Parametric Instabilities

G. DIPESO AND E. C. MORSE

Department of Nuclear Engineering,
University of California, Berkeley, California 94720

AND

R. W. ZIOLKOWSKI*

University of California,
Lawrence Livermore National Laboratory,
Livermore, California 94550

Received March 23, 1990; revised August 30, 1990

The δf and particle simulation methods are presented and compared for parametric instabilities in a 1D unmagnetized plasma. The δf simulation method used here is based on the linearized Vlasov equation. The simulation growth rates from both methods roughly agree with growth rates obtained from a fluid theory. Doubling the number of characteristics in the δf simulations does not significantly alter the growth rates. Doubling the number of particles in the particle simulation does alter the growth rates indicating that particle noise is interfering with the physics. The δf simulation method was also compared to Vlasov theory for parametric instabilities in a 1D magnetized plasma. The simulations generally agree with the theory.

1. INTRODUCTION

The theory of parametric instabilities has been developed for homogeneous plasmas [1–3] and inhomogenous plasmas [4, 5]. Computer simulation has been used to study parametric instabilities in homogeneous plasmas [6, 7], both magnetized and unmagnetized. Many theoretical calculations require simplifying assumptions to develop tractable dispersion relations. For example, Porkolab assumed relatively weak coupling in his derivation of a dispersion relation for parametric instabilities in a homogenous, magnetized plasma [2]. Tractable dispersion relations are necessary if one wants to study more complicated cases such as instabilities in the presence of plasma inhomogeneities [5]. Computer simulations do not require such assumptions and can be readily extended to more complicated cases such as a lower hybrid pump propagating through a compact torus [8].

δf simulation is a relatively new method that has been used to reduce stochastic orbit effects in linearized FRC tilt mode simulations [9] and to reduce particle

* Present address: University of Arizona, Tucson, AZ 85721.

0021-9991/91 $3.00

noise in simulations with realistic fusion parameters [10]. δf simulation methods reduce the noise inherent in particle simulations by solving for the perturbed portion of the δf equation along characteristics determined by the particle orbits. The δf's are then used to find densities and currents on a grid in space similar to the way particles are used in a particle simulation. Hence δf simulations are not to be confused with the solution of the Vlasov equation on a grid in x–v space [11].

Here, δf simulation is compared to particle simulation and fluid theory for ion acoustic parametric instabilities in an unmagnetized plasma. Since δf simulation is found to work better than particle simulation, it is also compared to Vlasov theory for ion quasimode parametric instabilities in a magnetized plasma. Note that for both these instabilities, there are associated purely growing modes which are also simulated. The results for the ion quasimode frequency show some departure from Porkolab's results at $k\lambda_{De} > 0.4$.

This article is divided into seven sections. In the second section, the dispersion relation and the δf and particle simulation equations for parametric instabilities in an unmagnetized plasma are presented. In the third section, the results of the dispersion relation and the simulations are given. In the fourth section, the equations for the δf simulation of a magnetized plasma are given and some generalizations to inhomogenous and collisional cases are made. In the fifth section, the method by which these equations are solved is presented. In the sixth section, the results of theory and simulation for parametric instabilities in 1D magnetized plasmas are given. In the seventh section, some concluding remarks are made and future code developments are suggested.

2. δf and Particle Simulation Equations

Consider a one-dimensional, infinite extent, non-relativistic, unmagnetized, spatially homogenous plasma equilibrium with a homogenous pump wave of the form $E_0 = \varepsilon \cos(\omega_0 t)$. A linear dispersion relation has been derived for the excited or daughter waves using a warm two fluid ($s = e, i$) model of the plasma and the Poisson equation for the electrostatic field response [1]:

$$\begin{aligned}(\omega^2 - \omega_i^2 + 2i\omega\Gamma_i)&((\omega_0 - \omega)^2 \\ &- \omega_e^2 - 2i(\omega_0 - \omega)\,\Gamma_e)((\omega_0 + \omega)^2 - \omega_e^2 + 2i(\omega_0 + \omega)\,\Gamma_e) \\ &- \frac{1}{4} k^2 \varepsilon^2 \frac{m_e}{m_i}((\omega_0 - \omega)^2 + (\omega_0 + \omega)^2 - 2\omega_e^2 + 4i\Gamma_e) = 0, \end{aligned} \tag{1}$$

where $\omega = \omega_R^l + i\omega_I$ and superscript l indicates a daughter wave with a frequency near the ion acoustic frequency. ω_e is the Langmuir frequency, ω_i is the ion acoustic frequency, and Γ_s is a Landau damping term added ad hoc to the fluid theory. All of these terms depend on the wave number k. ω, ω_0, ω_s, Γ_s are normalized by ω_{pe}, k is normalized by λ_{De}, and $\varepsilon_0 \varepsilon^2/2$ is normalized by $n_0 m_e v_{te}^2/2$. Note that all excited

modes grow with ω_I. A graph of ω_I vs k contains a branch for the ion acoustic parametric instability and another branch for the purely growing modes. This is shown by the theory line on Fig. 3.

Simulation equations based on the previous physical picture can be used to include kinetic effects directly without resorting to ad hoc damping. Furthermore, the nonresonant kinetic effects will be resolved and there is no need to develop a closure for the fluid equations. The δf and particle simulation equations will now be presented in greater detail since it is a new method.

The 1D Vlasov–Poisson model of a two species plasma is

$$\partial_t f_s + v\partial_x f_s + \frac{q_s}{m_s}(E_0 + E)\,\partial_v f_s = 0, \tag{2}$$

$$E = -\partial_x \phi, \tag{3}$$

$$\partial_x^2 \phi = -\frac{1}{\varepsilon_0}\sum_s \rho_s = -\frac{1}{\varepsilon_0}\sum_s q_s \int_{-\infty}^{\infty} dv f_s, \tag{4}$$

where E_0 is again the pump wave. Since the plasma is neutral without perturbations, the response terms ϕ, E, and ρ_s are due to the daughter waves and will now be known as $\delta\phi$, δE, and $\delta\rho_s$. Now, f_s is written as

$$f_s = f_{0s}(v) + \delta f_s(x, v, t). \tag{5}$$

Substituting the above form of f_s into the Vlasov equation and ignoring δf terms gives equilibrium and linearized perturbed equations:

$$\partial_t f_{0s} + \frac{q_s}{m_s} E_0 \partial_v f_{0s} = 0, \tag{6}$$

$$\partial_t \delta f_s + v\partial_x \delta f_s + \frac{q_s}{m_s} E_0 \partial_v \delta f_s = -\frac{q_s}{m_s}\delta E \partial_v f_{0s}. \tag{7}$$

The solution of Eq. (6) is simply

$$f_{0s}(v) = C \exp\left[-\frac{1}{2v_{ts}^2}\left(v - \frac{q_s}{m_s}\frac{\varepsilon}{\omega_0}\sin(\omega_0 t)\right)^2\right], \tag{8}$$

where the Maxwellian form of the solution is used and C is a normalization constant.

The δf simulation method solves Eq. (7) along the nth characteristic or unperturbed orbit:

$$\dot{x}_{sn} = v_{sn}, \tag{9}$$

$$\dot{v}_{sn} = \frac{q_s}{m_s} E_0. \tag{10}$$

The nth δf_s is modified along the nth characteristic as

$$\delta \dot{f}_{sn} = -\frac{q_s}{m_s} \delta E(x_{sn})\, \partial_v f_{0s}(v_{sn}), \tag{11}$$

where $\delta E(x_{sn})$ is weighted from a grid in space to the characteristic and $\partial_v f_{0s}(v_{sn})$ is known analytically.

Next, $\int dv\, \delta f_s$ is computed on a grid to solve the Poisson equation. At the jth grid point

$$n_{sj} = \frac{1}{\Delta x} \int_{x_j} dx \int dv f_s. \tag{12}$$

Note that the integration over v is understood to be from $-\infty$ to ∞. At $t=0$, $f = f_{0s}$, $n_s = n_{0s} = n_0$ (initially neutral plasma). The integral is approximated by a sum as

$$n_0 = \frac{1}{\Delta x} \int_{x_j} dx \int dv f_{0s} = \frac{1}{\Delta x} \sum_{n,j} dA_{sn} W_j(x_{sn}) f_{0sn}, \tag{13}$$

where dA_{sn} is a small piece of phase space area associated with the nth characteristic of species s.

The summation is done over all characteristics that contribute to the density at j and W is a normalized weighting from the characteristic to the grid. Let $\sum_{n,j} W_j = N_{csj}$, where N_{csj} is the number of characteristic of species s initially contributing information to grid point j. Then

$$dA_{sn} = \frac{\Delta x n_0}{f_{0sn} N_{csj}}. \tag{14}$$

dA_{sn} is a constant phase space area by Liouville's theorem. At $t>0$, the integrals in the Poisson equation are approximated by

$$\frac{1}{\Delta x} \int_{x_j} dx \int dv\, \delta f_s = \frac{n_0}{N_{csj}} \sum_{n,j} W_j(x_{sn}) \left(\frac{\delta f_s}{f_{0s}}\right)_n. \tag{15}$$

Note that integrating $(\delta f/f_0)_n$ may be achieved by dividing Eq. (11) by f_{0sn} which is a constant of motion along the characteristics given by Eqs. (9) and (10). Poisson's equation is then solved for $\delta\phi$ and a finite difference technique is used to find δE. The infinite extent plasma allows the use of periodic boundary conditions.

Standard methods of particle simulation proceed by following particles along their exact orbits:

$$\dot{x}_{sn} = v_{sxn}, \tag{16}$$

$$\dot{v}_{sxn} = \frac{q_s}{m_s} (E_0 + \delta E(x_{sn})), \tag{17}$$

where in Eq. (17), $\delta E(x_{sn})$ is again computed by weighting δE defined on a grid in space to the particle position x_{sn}. Then, the perturbed electron density is formed on the grid in space:

$$\delta\rho_{sj} = \frac{q_s}{\Delta x} \sum_{n,j} W_j(x_{sn}), \tag{18}$$

where W_j is a normalized weighting from the particle to the grid. Poisson's equation is again solved for $\delta\phi$ and a finite difference technique is again used to find δE.

Both methods can be generalized to multidimensional magnetized inhomogenous plasmas. δf simulation need not be linearized [10] although it is more easily linearized than particle simulation [9]. One disadvantage of δf simulation is that there is one extra equation per characteristic (particle), i.e., the evolution of δf. Another disadvantage of δf simulation is that f_0 may not be analytically known making it difficult to calculate the velocity derivatives of f_0 necessary to advance δf as in Eq. (11). This will be elaborated upon in Section 4. The advantage of δf simulation is that it has better signal to noise characteristics since δf is solved directly. At this time, there is no rigorous proof of this effect.

Particle simulation of the parametric instability was done using ES1, a standard particle simulation program for 1D electrostatic plasmas [12]. In these simulations, particles were initially loaded uniformly in space and Maxwellian in velocity using the quiet start technique. The orbit equations were integrated using a leapfrog mover and the Poisson equation was solved using fast Fourier transforms. The instabilities were started in ES1 by a small sinusoidal displacement in particle position which produced a small δE at $t = 0$.

δf simulation of the parametric instabilities was done using PAR1, which is based on ES1, but solves the $(\delta f/f_0)_n$ equations instead of the orbit equations. The equations were integrated using an explicit Euler scheme. A time centered method for the magnetized simulations will be presented in Section 5. The characteristic equations were solved analytically for the present model. The characteristics were loaded as the particles were loaded in ES1 and the Poisson equation was solved using the same routine. PAR1 is normalized according to the normalizations introduced for Eq. (1) and equivalent input parameters were calculated for ES1. The instabilities in PAR1 were started by a small sinusoidal displacement in the δf's to produce an identical δE at $t = 0$.

3. Instability Results: 1D Unmagnetized Plasma

The instability was simulated for the parameters $T_e/T_i = 30$, $m_e/m_i = 0.001$, $\omega_0 = 1.04$, $\varepsilon = 0.5$, and $0.07 \leqslant k \leqslant 0.25$ in normalized units (cf. Eq. (1)). The system length was taken to be equal to the wavelength corresponding to each k. Figures 1 and 2 show particular simulations at $k = 0.13$ and $k = 0.19$. The ES1 signal in time domain was taken from the mode 1 field energy, since the total field energy was

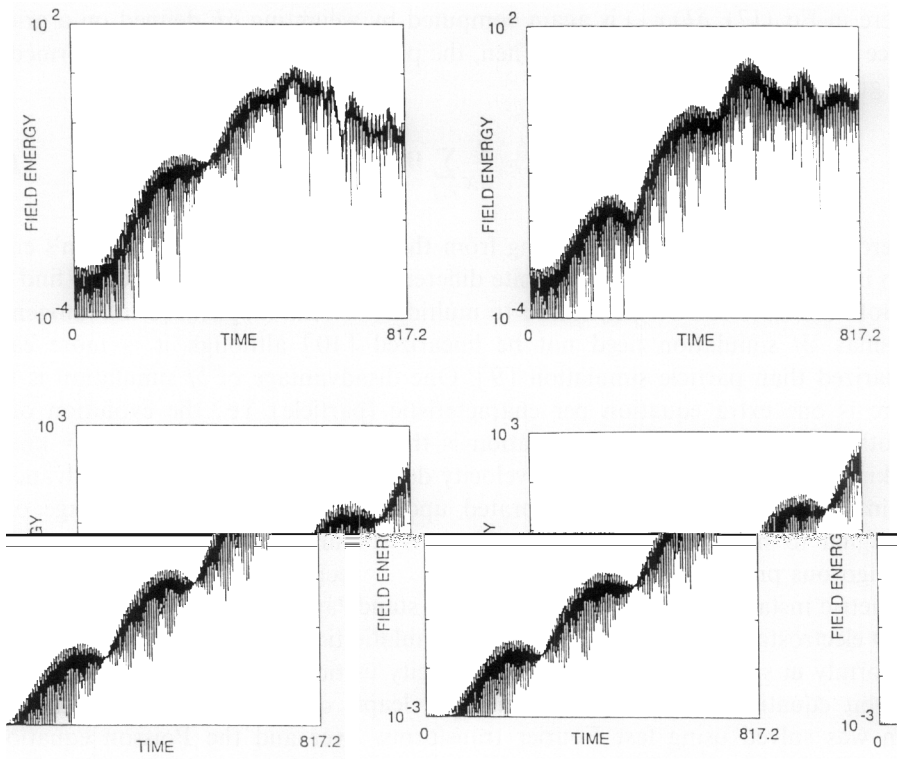

FIGURE 1

very noisy making it difficult to measure the growth rate of the instability. The PAR1 signal in time domain was taken from the total field energy. For both figures, the ES1 simulations appear to change more than the PAR1 simulations as the number of particles (characteristics) is doubled. The noise in the ES1 simulations appears at the onset of instability, i.e., at the point where one measures the linear growth rate, and at the nonlinear saturation of the instability. This indicates that PAR1 gives a cleaner picture of the instability and the noise in ES1 occurs in the linear and nonlinear stages of the instability and is due to the particles. The amplitude of δE for all starting perturbations was 0.01. Smaller perturbations gave noisy results in ES1 at the onset of instability making even mode 1 field energy measurements difficult.

Figure 3 gives the growth rates for the various k. In simulations for $k \geqslant 0.13$, the number of grids cells was 256. Runs were made with 8192 and 16,384 particles (characteristics). For $k < 0.13$, the number of grids and particles (characteristics) were doubled in all runs to accommodate longer system lengths associated with the smaller k. All simulations were run for 4096 time steps of length 0.2. The theory curve was drawn using Eq. (1).

ES1 and PAR1 simulations agree roughly with theory and show purely growing

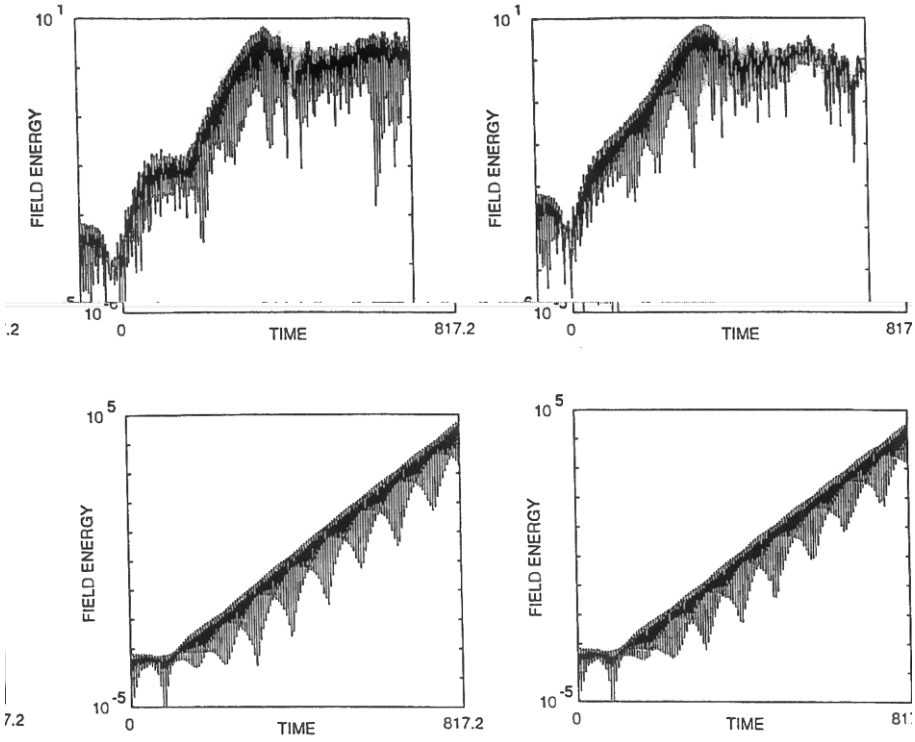

FIGURE 2

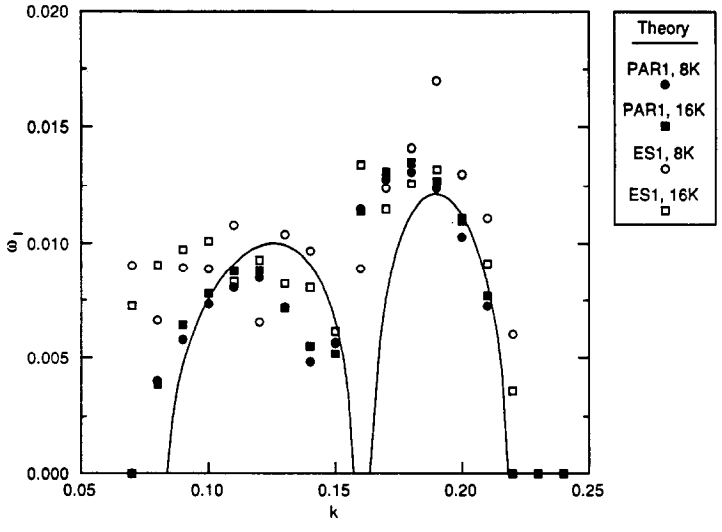

FIGURE 3

modes at $k > 0.15$. The ES1 simulation growth rates change for doubled particles whereas the PAR1 simulation growth rates remain about the same for doubled characteristics. It should be noted that the theory is based on a fluid model with resonant kinetic effects added in ad hoc so exact agreement between theory and kinetic simulations should not be anticipated.

4. δf Simulation Equations for a Magnetized Plasma

The δf simulation equations will be presented for the physical model shown on Fig. 4. For this 1D 3-v model, $\mathbf{x} = (x, 0, 0)$ and $\mathbf{v} = (v_x, v_y, v_z)$. The external magnetic field has a tilt $\mathbf{B}_0 = (B_{0x}, 0, B_{0z})$ so that $k_\perp$ and $k_{||}$ are included. Relativistic and collisional effects are ignored. The response to the pump wave is assumed to be electrostatic. The homogeneous plasma has infinite extent implying periodic boundary conditions for the solution of the Poisson equation. The Vlasov–Poisson model of a two species plasma is

$$\partial_t f_s + v_x \nabla_{\mathbf{x}} f_s + \frac{q_s}{m_s} (\mathbf{E}_{pmp} + \mathbf{E} + \mathbf{v} \times \mathbf{B}_0) \cdot \nabla_{\mathbf{v}} f_s = 0, \tag{19}$$

$$\mathbf{E} = (E_x, 0, 0) = -\nabla_{\mathbf{x}} \phi, \tag{20}$$

$$\nabla_{\mathbf{x}}^2 \phi = -\frac{1}{\varepsilon_0} \sum_s \rho_s = -\frac{1}{\varepsilon_0} \sum_s q_s \int_{\mathbf{v}} \mathbf{dv} f_s, \tag{21}$$

where $\mathbf{E}_{pmp}$ is the pump wave. For the dipole pump of Fig. 4, $\mathbf{E}_{pmp} = (0, E_{0y} \cos(\omega_0 t), 0)$.

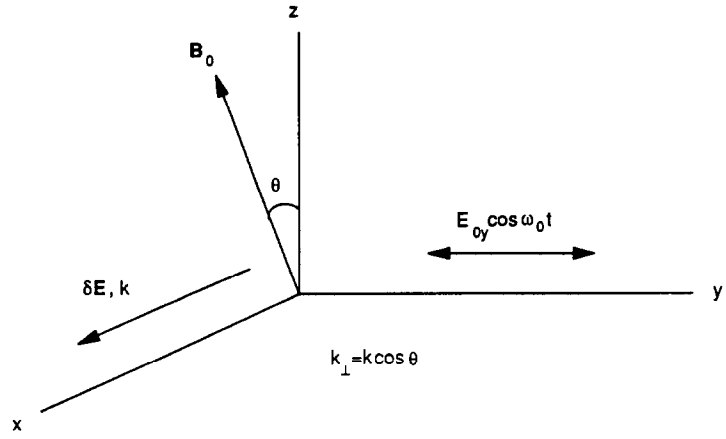

Figure 4

Since the plasma is neutral without perturbations, the response terms ϕ, $\mathbf{E}$, and ρ_s are due to the daughter waves and will now be known as $\delta\phi$, $\delta\mathbf{E}$, and $\delta\rho_s$. Now, f_s is written as

$$f_s = f_{0s}(\mathbf{v}) + \delta f_s(\mathbf{x}, \mathbf{v}, t). \tag{22}$$

Substituting the above form of f_s into the Vlasov equation and ignoring $\delta\delta$ terms gives equilibrium and perturbed equations:

$$\partial_t f_{0s} + \frac{q_s}{m_s}(\mathbf{E}_{pmp} + \mathbf{v}\times\mathbf{B}_0)\cdot\nabla_{\mathbf{v}} f_{0s} = 0, \tag{23}$$

$$\partial_t \delta f_s + v_x \nabla_{\mathbf{x}} \delta f_s + \frac{q_s}{m_s}(\mathbf{E}_{pmp} + \mathbf{v}\times\mathbf{B}_0)\cdot\nabla_{\mathbf{v}}\delta f_s = -\frac{q_s}{m_s}\delta\mathbf{E}\cdot\nabla_{\mathbf{v}} f_{0s}. \tag{24}$$

The $\nabla_{\mathbf{x}} f_{0s}$ term is missing from Eq. (23) because of the assumed homogeneity.

The δf simulation method solves Eq. (24) along the nth characteristic or unperturbed orbit:

$$\dot{\mathbf{x}}_{sn} = \mathbf{v}_{sn}, \tag{25}$$

$$\dot{\mathbf{v}}_{sn} = \frac{q_s}{m_s}(\mathbf{E}_{pmp} + \mathbf{v}_{sn}\times\mathbf{B}_0). \tag{26}$$

The nth δf_s is modified along the nth characteristic as

$$\delta\dot{f}_{sn} = -\frac{q_s}{m_s}\delta\mathbf{E}(\mathbf{x}_{sn})\cdot\nabla_{\mathbf{v}} f_{0s}(\mathbf{v}_{sn}), \tag{27}$$

where $\delta\mathbf{E}(\mathbf{x}_{sn})$ is weighted from a grid in space to the characteristic. Due to the homogeneity of $\mathbf{B}_0$ and $\mathbf{E}_{pmp}$, the characteristic Eqs. (25) and (26) can be solved analytically. For inhomogenous plasmas and pumps, these equations can be solved numerically.

If at $t=0$, $f_{0s}(\mathbf{v}) = F_s(\mathbf{v})$, where F_s is a Maxwellian, then the solution of Eq. (23) is

$$f_{0s}(\mathbf{v}) = F_s(\mathbf{v} - \mathbf{v}_d), \tag{28}$$

where $\mathbf{v}_d$ is the time dependent velocity drift due to $\mathbf{E}_{pmp}$. With f_{0s} analytically known, $\nabla_{\mathbf{v}} f_{0s}$ may be evaluated for any $\mathbf{v}$ at any t. For inhomogenous plasmas and pumps, an analytic solution for f_{0s} and hence $\nabla_{\mathbf{v}} f_{0s}$ will usually not exist even if f_{0s} is known analytically at $t=0$. It may be possible to construct some analytic form for $\nabla_{\mathbf{v}} f_{0s}$ or it may be necessary to solve the derivatives of Eq. (23) numerically. Applying $\nabla_{\mathbf{v}}$ and $\nabla_{\mathbf{x}}$ to Eq. (23) (with the $\nabla_{\mathbf{x}} f_{0s}$ term restored) will generate equations which may then be solved numerically along the characteristics to obtain $\nabla_{\mathbf{v}} f_{0s}$.

Next, the perturbed particle density is computed on the grid as outlined in Section 2. Collisional effects may be added by modifying dA_{sn} some appropriate way and adding a collisional term to Eq. (24). Poisson's equation is then solved for $\delta\phi$ and a finite difference technique is used to find $\delta\mathbf{E}$. δf simulation of the parametric instabilities for the model on Fig. 4 was done using the code PARM which is based on PAR1 introduced in Section 2. In the next section, the numerical details of the PARM code are discussed.

5. Method of Solution

The δf evolution Eq. (27) may be written as

$$\left(\frac{\delta \dot{f}_s}{f_{0s}}\right)_n = -\frac{q_s}{m_s}\,\delta E_x(x_{sn})\,\frac{\partial_{v_x} f_{0s}}{f_{0s}}(\mathbf{v}_{sn}); \tag{29}$$

x_{sn} and $\mathbf{v}_{sn}$ are known analytically, but $(\delta f/f_0)_n$ must be pushed. A time centered trapezoidal push from time step m to $m+1$ based on Eq. (29) is given by

$$\left(\frac{\delta f_s}{f_{0s}}\right)_n^{m+1} = \left(\frac{\delta f_s}{f_{0s}}\right)_n^{m} + \frac{\Delta t}{2}\,\delta E_x^m(x_{sn}^m)\,g_s^m(\mathbf{v}_{sn}^m) + \frac{\Delta t}{2}\,\delta E_x^{m+1}(x_{sn}^{m+1})\,g_s^{m+1}(\mathbf{v}_{sn}^{m+1}), \tag{30}$$

where $g_s(\mathbf{v}_{sn}) = -(q_s/m_s)\,\partial_{v_s} f_{0s}/f_{0s}(\mathbf{v}_{sn})$ is known analytically.

Substituting Eq. (30) into the Poisson equation at grid point j, time step $m+1$ gives

$$\partial_{xj}^2 \delta\phi^{m+1} = -\frac{1}{\varepsilon_0}\sum_s q_s\left(\frac{n_0}{N_{csj}}\sum_{n,j} W_j(x_{sn}^{m+1})\,\chi_{sn}^m\right) - \frac{1}{\varepsilon_0}\sum_s q_s\left(\frac{n_0}{N_{csj}}\frac{\Delta t}{2}\sum_{n,j} W_j(x_{sn}^{m+1})\,\delta E_x^{m+1}(x_{sn}^{m+1})\,g_s^{m+1}(\mathbf{v}_{sn}^{m+1})\right), \tag{31}$$

where χ_{sn}^m is the explicit part (m terms) of Eq. (30).

Using nearest grid point (NGP) weighting from the characteristic to the grid and the grid to the characteristic, $W_j = 1.0$ and the time step $m+1$ field that pushes any particular $(\delta f/f_0)_n$ comes from a grid point to which that $(\delta f/f_0)_n$ will be weighted. The δE term in Eq. (31) may be then removed from $\sum_{n,j}$ making the iterations easier. If linear weighting was used, the δE term could still be removed, but then there would be $\sum_{n,j}$, $\sum_{n,j+1}$, and $\sum_{n,j-1}$ terms. For two spatial dimensions, there would be 10 summations. One drawback to NGP is that it is noisier than linear weighting. Another drawback is that NGP is of order 1. The Poisson solver, accurate to Δx^2, and the δf solver, accurate to Δt^2, are both of order 2 but the use

of NGP to couple these equations together may reduce overall accuracy. However, the faster NGP method is used.

Equation (31) then becomes an iterative Poisson equation:

$$\partial_{xj}^2 \delta\phi^{m+1} = -\frac{1}{\varepsilon_0}\sum_s q_s \left(\frac{n_0}{N_{csj}} \sum_{n,\, j = x_{sn}^{m+1}} \chi_{sn}^m + \frac{n_0}{N_{csj}} \frac{\Delta t}{2} \delta E_{xj}^{m+1} \sum_{n,\, j = x_{sn}^{m+1}} g_s^{m+1}(\mathbf{v}_{sn}^{m+1}) \right). \tag{32}$$

This can be solved iteratively in conjuction with the definition $\delta E_x = -\partial_x \delta\phi$.

The sequence to advance the system of equations would then be:

- Advance the characteristics.
- Calculate the sums on the RHS of Eq. (32).
- Iteratively solve Eq. (32) and the defining equation for δE_x. Typically only two or three iterations are necessary for convergence. The δE_x at the previous time step is used as an initial guess.
- Advance χ_{sn}.

6. Instability Results: 1D Magnetized Plasma

The instabilities were simulated for the parameters $T_e/T_i = 3$, $m_e/m_i = 5.43 \times 10^{-4}$, $\omega_0 = 0.0282$, $\omega_{ce} = 1.71$, $E_{0y} = 0.120$, and $0.05 \leqslant k \leqslant 0.6$ in normalized units (cf. Eq. (1)). The system length was taken to be equal to the wavelength corresponding to each k. Figure 5 illustrates simulations for $k = 0.3$ (ion quasimode) and $k = 0.15$ (purely growing mode). The signal in time domain for PARM is taken from the field energy. For the ion quasimode, the frequency spectrum shows the lower sideband and the ion quasimode frequencies as peaks from right to left. For the purely growing mode, the frequency spectrum shows only a frequency near the pump as the center peak.

Figure 6 contains the results of the simulations. For all runs, the time step was 1.0. For $k > 0.2$, 8192 characteristics per species and 256 grid cells were used. For $k < 0.2$, longer wavelengths needed to be resolved. Hence, the number of grid cells and the number of characteristics were both quadrupled. Figure 6 also contains the results from theory, i.e., the results from Fig. 3b of Ref. [3]. The derivation of this theory is well described in Refs. [2, 3] and, like the simulations, is based on the Vlasov–Poisson system of equations.

A disagreement between simulation and theory occurs for $k \gtrsim 0.4$. In this range, simulation indicates that the ion quasimode frequency remains locked at $\omega_R/\omega_0 = 0.206$, where as theory says, that the frequency should decrease. To check the simulations, runs were made with a time step of 0.5, 1024 grid cells, and 49,152 characteristics per species for $k = 0.5$ shown on Fig. 7 and for $k = 0.6$ shown on

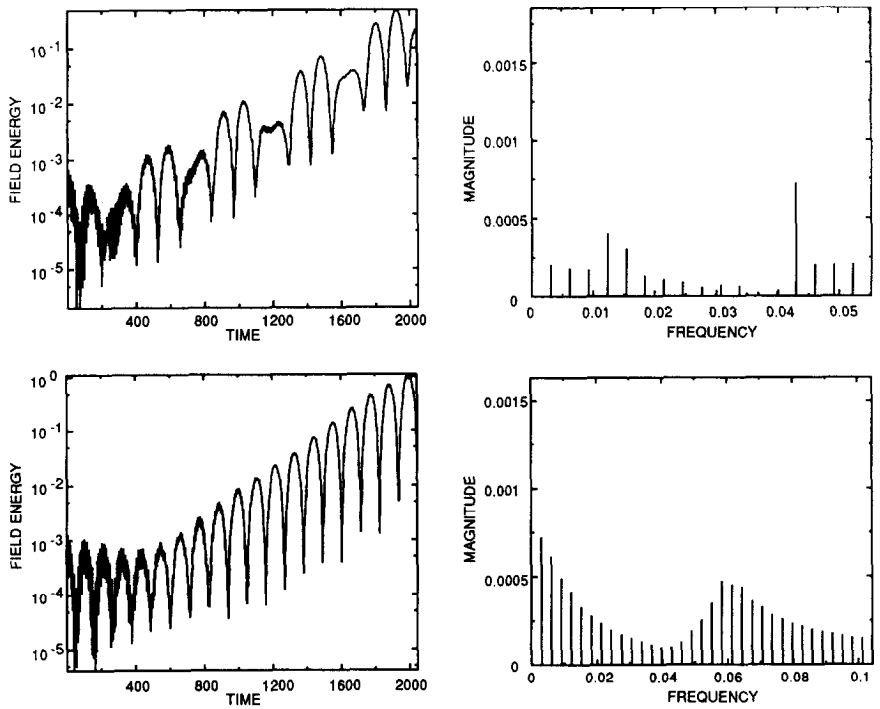

FIGURE 5

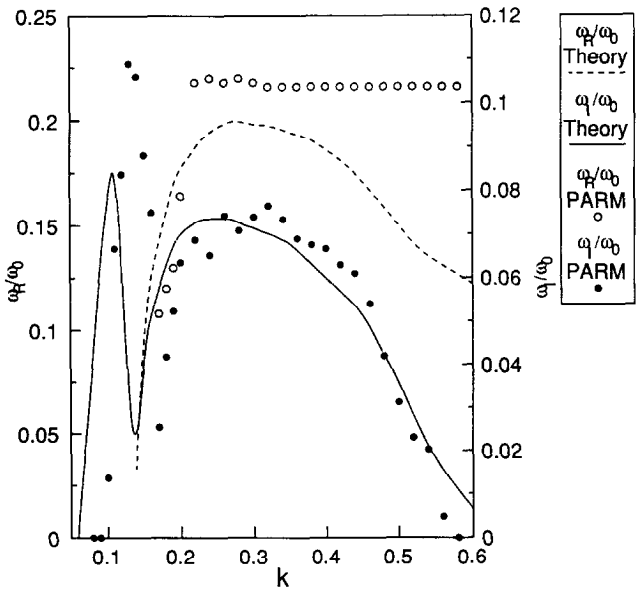

FIGURE 6

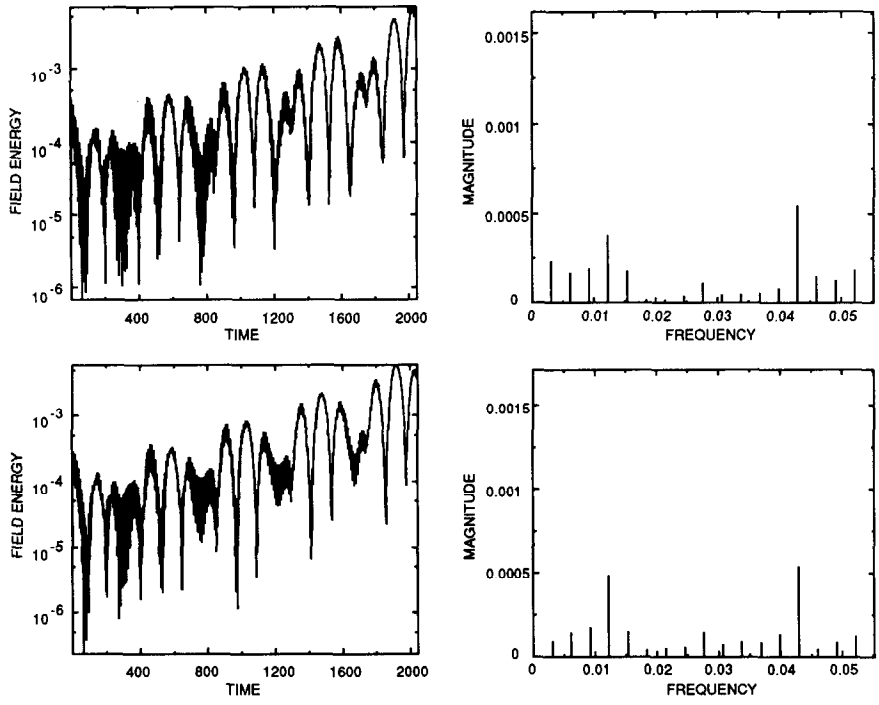

FIGURE 7

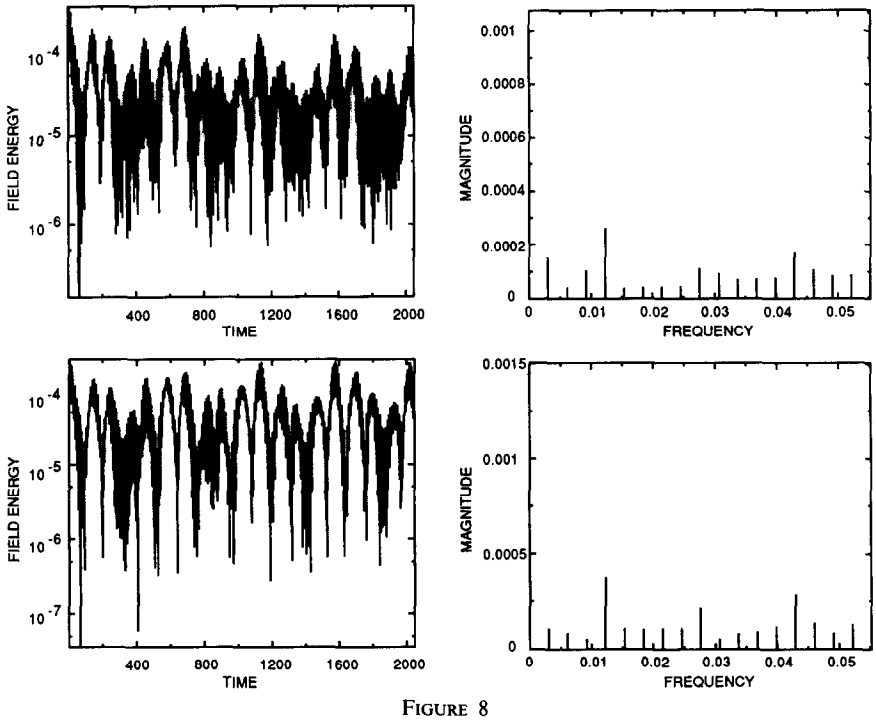

FIGURE 8

Fig. 8. These results are similar to the results used to produce the $k = 0.5$, 0.6 points on Fig. 6 (these runs are also shown on Figs. 7 and 8). The theory is valid for any k up to and including $\mu \sim 1$, where $\mu = E_{0y}k/(\omega_{ce}\omega_0)$ is the coupling coefficient defined in Ref. [3] but recast in normalized units (cf. Eq. (1)). For the parameters used in the simulation, $\mu > 1$ for $k > 0.4$ so the theory should be valid. It should be noted that, although there is a discrepancy in the ion quasimode frequency, the quasimode growth rates given by theory and simulation agree well.

7. Conclusion

δf and particle simulations have been compared to theory for parametric instabilities in a 1D unmagnetized plasma. There is a rough agreement between theory and simulation but this may be expected, since the theory is basically a fluid model. The δf simulations give a cleaner picture of the instabilities and were therefore used to simulate parametric instabilities in a 1D magnetized plasma. For this case, the simulations generally agreed with theory since the theory is a Vlasov–Poisson model.

Ultimately, a δf simulation code for plasma response will be tied into a ray tracing code for the pump wave propagation. In this manner, the onset of parametric instabilities can be studied in more complicated situations such as the heating of compact toroids with Gaussian pulsed RF around the lower hybrid frequency. The difficulty in using δf simulation is the lack of an analytic f_0. The brute force method outlined in Section 4 to overcome this problem may be numerically prohibitive. However, a particle method may also be numerically prohibitive in that a large amount of particles would be needed to overcome statistical noise in order to clearly see the competing effects of a moving pump wave and plasma and pump wave inhomogeneities. A computational cost comparison between δf and particle simulation should be done to verify savings in CPU time in using δf simulation versus particle simulation with the condition that both codes achieve the same effectiveness.

References

1. K. Nishikawa, *J. Phys. Soc. Jpn.* **24**, 916, 1152 (1968).
2. M. Porkolab, *Phys. Fluids* **17**, 1432 (1974).
3. M. Porkolab, *Phys. Fluids* **20**, 2058 (1977).
4. M. N Rosenbluth, *Phys. Rev. Lett.* **29**, 565 (1972).
5. E. A. Williams, *Phys. Rev. Lett.* **59**, 2709 (1987).
6. W. L. Kruer and J. M. Dawson, *Phys. Fluids* **15**, 446 (1972).
7. J. M. Kindel, H. Okuda, and J. M. Dawson, *Phys. Rev. Lett.* **29**, 995 (1972).
8. E. C. Morse and R. W. Ziolkowski, *Fusion Technol.* **14**, 1325 (1988).
9. Z. Mikic and E. C. Morse, *Phys. Fluids* **30**, 2806 (1987).
10. M. Kotschenreuther, *Bull. Am. Phys. Soc.* **33**, 2109 (1988).
11. J. Denavit, *J. Comput. Phys.* **9**, 75 (1972).
12. C. K. Birdsall and A. B. Langdon, *Plasma Physics via Computer Simulation* (McGraw–Hill, New York, 1985).